Diagnostics of pillars in St. Mary's Church (Gdańsk, Poland) using the GPR method

Jacek Lachowicz*, Magdalena Rucka

Department of Mechanics of Materials and Structures
Faculty of Civil and Environmental Engineering
Gdańsk University of Technology
ul. Narutowicza 11/12, 80-233 Gdańsk, Poland
email: jacek.lachowicz@pg.edu.pl, magdalena.rucka@pg.edu.pl
**corresponding author*

Abstract

The main goal of this study was non-destructive evaluation of pillars in the St. Mary's Church (Gdańsk, Poland) using the ground penetrating radar (GPR) technique. The GPR inspection was conducted on four brick masonry pillars and five pillars strengthened by reinforced concrete jacketing. Data were acquired with a 2 GHz antenna along longitudinal and transverse profiles. The study involved the estimation of the electromagnetic wave velocity in both brick and concrete, the inspection of the internal structure of the pillars and the precise identification of reinforcement bars. To determine the wave velocity in bricks, a novel mathematical model was developed. Finite-difference time-domain (FDTD) simulations were used to verify and assess the feasibility of the proposed model. Finally, GPR maps were processed using the hyperbolic summation method to visualize the reinforcement distribution in the concrete jacket.

Keywords

ground penetrating radar; non-destructive testing; historical buildings; masonry pillars; strengthening; reinforced concrete jacketing; velocity estimation

1. Introduction

A large number of historical monuments contain brick or stone masonry. Monuments, due to their great importance to architectural heritage, require effective non-destructive testing (NDT) methods for condition assessment. Among various NDT approaches (e.g., (Zendri et al. 2017; Sfarra et al. 2015)), ultrasonic and electromagnetic wave propagation techniques are of great importance in the diagnostics of masonry structures. The ultrasonic method is a powerful tool for tomographic imaging to reproduce the internal structure of masonry pillars (Binda, Saisi, and Zanzi 2003), piers (Binda et al. 2003), and columns (Pérez-Gracia et al. 2013; Santos-Assunçao et al. 2014). The results obtained from ground penetrating radar (GPR) surveys have enabled the identification of air voids and unfilled joints in brick masonry walls (Maierhofer and Leipold 2001; Hamrouche et al. 2012), defects in masonry columns due to compression (Santos-Assunçao et al. 2014) and moisture distribution in brick masonry walls (Lai et al. 2014), (Cetrangolo et al. 2017). In previous research, the GPR method has been successfully applied in diagnostics of many historical structures, e.g., the Church of S. Nicolò l'Arena in Catania (Italy) (Binda, Saisi, and Zanzi 2003), the Noto Cathedral in Sicily (Italy) (Binda et al. 2003), the Bell Tower in Cremona (Italy) (Binda et al. 2005), a Romanesque bridge in Fillaboa (Spain) (Pérez-Gracia et al. 2011), the S. Agata Cathedral of Catania (Italy) (Imposa and Mele 2011), the Cathedral of Saint Mary in Mallorca (Spain) (Pérez-Gracia et al. 2013), the Santa Maria di Collemaggio Church in L'Aquila (Italy) (Sfarra et al. 2015), the Cathedral of Tricarico (Italy) (Leucci et al. 2011), the Cathedral of Otranto (Italy) (Leucci, Cataldo, and De Nunzio 2007) and St. Mary's Church in Gdańsk (Poland) (Rucka, Lachowicz, and Zielińska 2016).

In this work, the GPR evaluation of masonry pillars in a historic church is presented. The GPR surveys were conducted on brick masonry pillars and pillars strengthened by reinforced concrete jacketing. Conducted investigations were focused on the precise identification of the velocity of electromagnetic waves because this parameter is crucial for the proper calculation of the distance scale and the proper evaluation of the internal pillar structure. Multiple previous works have focused on the estimation of the electromagnetic wave velocity. Numerous models use hyperbola fitting to assess the wave velocity in concrete (Hayakawa and Kawanaka 1998; Ristic, Petrovacki, and Govedarica 2009; Sham and Lai 2016; Persico et al. 2015), while estimating the velocity in masonry structures is generally performed using the "depth to known reflector" method (Stryk et al. 2015). In the present study, a novel method for identification of the velocity of electromagnetic waves in bricks

based on line fitting is developed. Velocities in both brick and concrete are determined, and GPR maps are used to assess the internal pillar structure. To accurately display the reinforcement distribution, the migration processing is conducted using the hyperbolic summation method.

2. Object of interest and problem description

St. Mary's Church (the Basilica of the Assumption of the Blessed Virgin Mary) located in Gdańsk (Poland) is one of the largest brick buildings used for religious purposes (Figure 1a). The main nave length is 105.2 m, and the width of the transept is 66.2 m. The vaults of the ceiling are supported by 26 masonry (brick), octagonal pillars (Figure 1b, Figure 2). The construction of the church began in 1343 and was executed in several stages over 150 years. Near the end of the Second World War, in 1945, the church was heavily damaged by aerial bombs and artillery shells and then by fire. All roofs and the interior of the church burned down, and approximately 40% of the vaults collapsed.

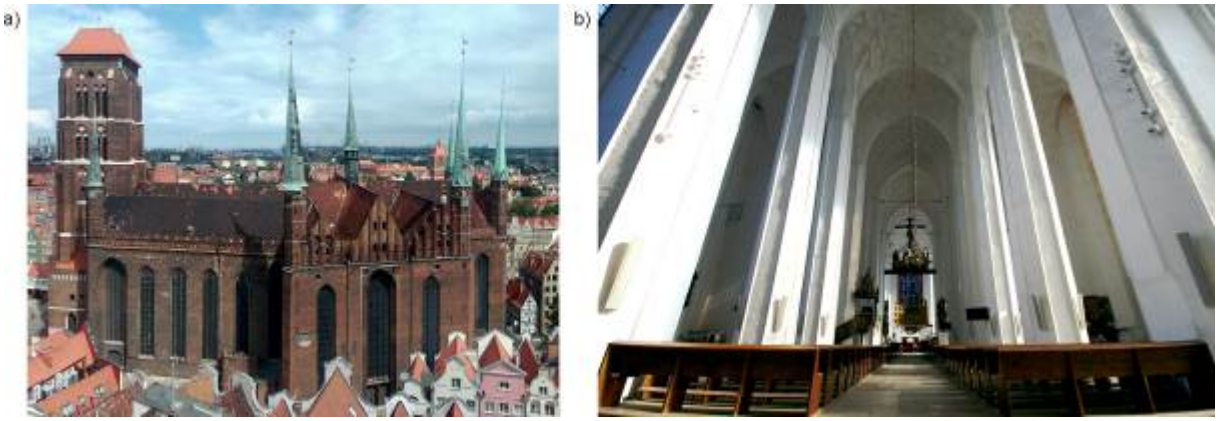

Figure 1. (a) Photograph of St. Mary's Church in Gdańsk, Poland (b) photograph of the church interior

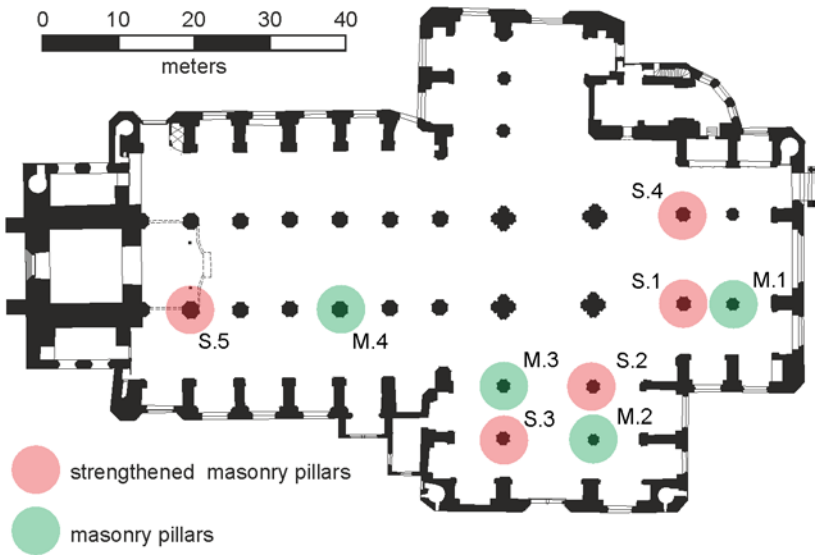

Figure 2. Plan view (redrawn after (Bogdanowicz 1990)) with locations of GPR surveys indicated

The rebuilding of the roof and vaults began in 1947. During reconstruction work, five pillars began to crack and tilted from the vertical (Bogdanowicz 1990). All damaged pillars were strengthened using a technique of jacketing (c.f. (Júlio, Branco, and Silva 2003)). In Figure 2, the reinforced pillars are indicated. As the first example, pillar S.1 was repaired in 1948 with the use of prefabricated elements (Figure 3a). Moulds were prepared, and 500 pieces of concrete cover with heights of 20 cm were fabricated. The pillar was then covered with the prefabricated elements over 3 months at a height of 18 m. One year later, cracks appeared on pillar S.4 during vault reconstruction. Damage started to propagate rapidly, and a horizontal crack emerged. In this situation, immediate reinforcement of the pillar was necessary, and monolithic reinforced concrete was used. The reinforcement of a cracked area was completed in 24 hours. The concreting was conducted in few stages, each with a section height of approximately 110-140 cm (Figure 3b). The remaining three pillars (S.2, S.3, and S.5) were also reinforced using monolithic concrete.

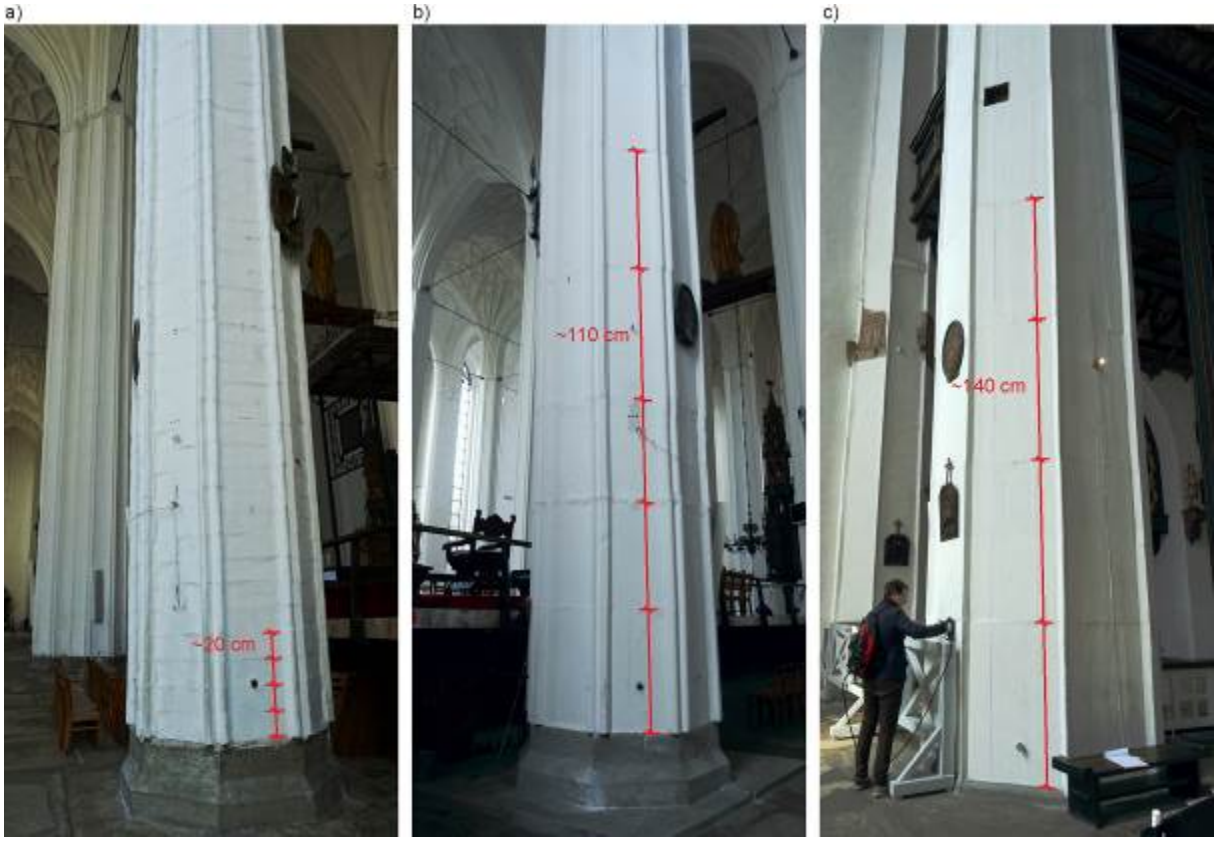

Figure 3. Strengthened pillars: a) pillar S.1; b) pillar S.4; c) pillar S.5

As in the case for many historical monuments, the availability of technical documentation from the past is limited. For example, in the case of St. Mary's Church, the only source of knowledge concerning pillar reconstruction are written memories of the reconstruction of the main city (Trojanowska 1997) and a sketch from a construction logbook

showing a reinforced concrete ring (Figure 4). An additional challenge is that the pillars are plastered. Only a few areas are open, allowing for observation of the inner structure of the pillars. Figure 5 gives two details showing masonry and reinforced masonry in two pillars. In such situations, visual inspection and NDT are the only suitable methods for diagnosis and assessment of the condition of the pillars.

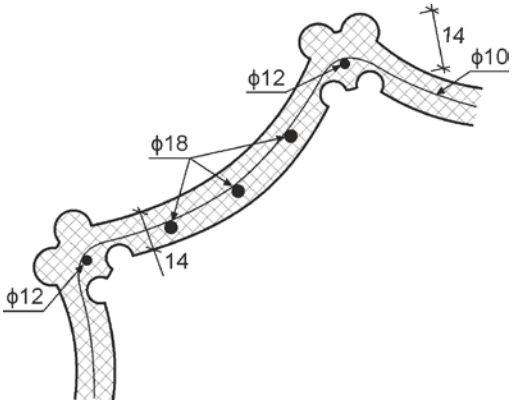

Figure 4. Sketch of a pillar strengthened by jacketing (redrawn after the construction logbook)

Figure 5. Plastered pillars with open areas showing details of masonry and reinforced masonry

3. Theoretical background

3.1. GPR wave velocity identification

The electromagnetic wave that encounters a circular inclusion with various electrical parameters from the tested medium diffracts, causing a hyperbola pattern on the GPR map, as shown in Figure 6a. The model of the hyperbola taking into account the radius R of reinforcement and the offset s between the receiving and transmitting antennas can be described as follows (Sagnard and Tarel 2016):

$$t = \frac{1}{v}\left(\sqrt{\left(\frac{vt_0}{2}+R\right)^2+\left(x_0-x_i-\frac{s}{2}\right)^2}+\sqrt{\left(\frac{vt_0}{2}+R\right)^2+\left(x_0-x_i+\frac{s}{2}\right)^2}-2R\right) \tag{1}$$

where t is the two-way travel time registered by the receiving antenna, x_0 is the location of the inclusion, x_i is the radar position, t_0 is the two-way travel time to the inclusion and v denotes the velocity of electromagnetic waves in the considered medium.

In the case of brick structures, the shapes occurring on GPR maps are reflections from vertical joints between bricks. The surface wave emitted from the transmitting antenna returns after reflection from the joint travelling along the same path; therefore, the wave retains the shape of a straight line with an inclination angle that contains information on the wave velocity in the tested medium (Figure 6b). The mathematical description of the reflection consists of the following simple relationship:

$$t = \frac{2\left(x_i - x_0\right)}{v} \tag{2}$$

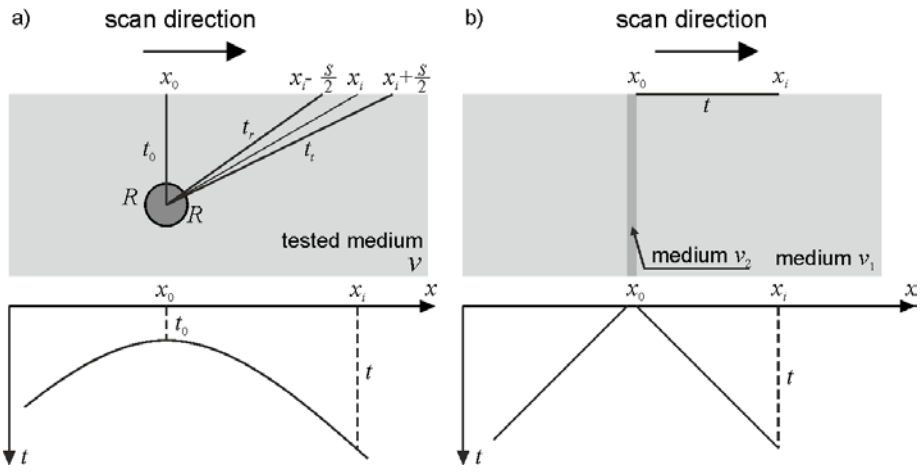

Figure 6. Reflection models in various types of structures:
a) reinforcing bar in concrete; b) vertical joint between bricks

3.2 Hyperbolic summation

A georadar antenna during the scan through the examined surface collects the reflected and scattered electromagnetic field to produce various imaging results on the GPR map. One such pattern is a hyperbola, as described in the previous section. To represent a circular object hidden behind the hyperbola, the hyperbolic summation method proposed by Özdemir (Özdemir, Demirci, and Yiğit 2008; Özdemir et al. 2014) was applied. Assuming that the antenna moves along the *X*-direction and emits and registers the signal in the *Z*-direction, a relationship describing the emerging hyperbola from the Pythagorean theorem can be written:

$$Z = \sqrt{z_0^2 + \left(X - x_0\right)^2} \tag{3}$$

The assumptions of the method are the homogeneity of the material and the fact that the antenna is directly adhered to the scanned surface. The algorithm was implemented in MATLAB® environment. In the first step, the time scale of the GPR map is converted into the distance scale, for which an estimation of the electromagnetic wave velocity is performed. Next, it is assumed that each point of the GPR map (x_i, z_i) can produce a hyperbola. Thus, at each point of the map, a hyperbola is defined according to Eq. (3), and then voltage values coinciding with the calculated formula are added (Figure 7). The value calculated in this way is saved on a new map. The algorithm repeats until all points of the entire B-scan are migrated from (x_1, z_1) to (x_n, z_n). The result of the migration process is a new GPR map containing a significant increase of the summed voltage values at the top of the hyperbola.

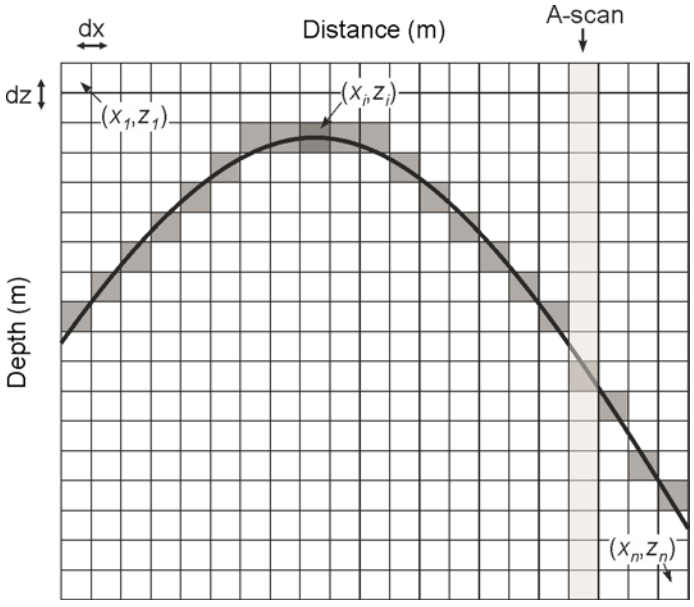

Figure 7. Scheme of the hyperbolic summation method

4. FDTD simulations

In GPR investigations, numerical modelling is often used as a tool for testing new data processing algorithms. In previous studies (e.g. (Hayakawa and Kawanaka 1998; Ristic, Petrovacki, and Govedarica 2009; Lachowicz and Rucka 2018; Leucci 2012)) various models using hyperboles to evaluate the velocity of electromagnetic waves in reinforced concrete structures were verified. In this paper, numerical analyses were used to verify and assess the feasibility of the proposed mathematical model for the identification of the electromagnetic wave velocity in brick structures.

Calculations were performed using the gprMax software (Warren, Giannopoulos, and Giannakis 2016) using the finite-difference time-domain (FDTD) method. Two numerical models were created. The first considered example was a concrete specimen with an embedded steel bar of 12 mm diameter (Figure 8a). The second model contained a vertical inclusion between two brick specimens (Figure 8b). Such model can be considered as a representation of a masonry structure in which the vertical inclusion is a mortar joint between bricks. The values of the relative permittivity of bricks (ε_r = 3.5) and concrete (ε_r = 7) were determined in accordance with velocities obtained from in-situ surveys. For the mortar, the value of the permittivity was set as ε_r = 5. The external dimensions of the models were 0.35 m × 0.6 m. The models were discretized using the grid with spatial steps of 0.001m × 0.001m. At the edges of the area, the perfectly match layer (PML) absorbing boundary conditions were set up. The Ricker function with a centre frequency of 2 GHz was used as a source. The distance between the transmitting and receiving antennas was set to 6 cm according to the applied IDS antenna.

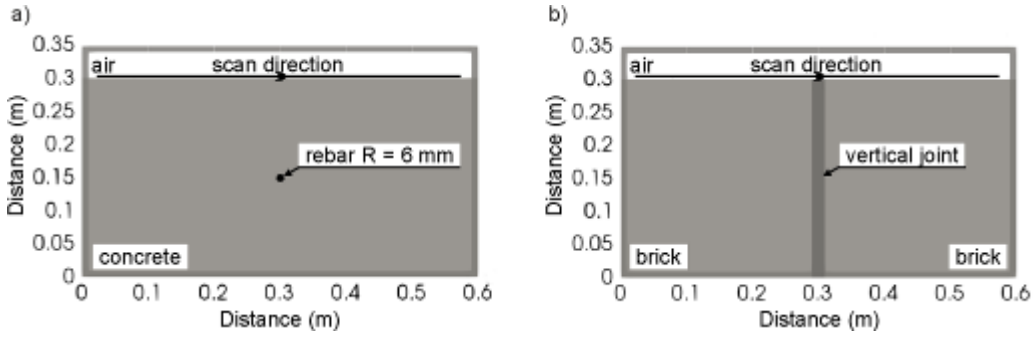

Figure 8. Numerical models: a) reinforcing bar in concrete; b) vertical joint between bricks

Figure 9 shows numerical GPR maps. A hyperbolic reflection can be seen on the radargram obtained for the concrete specimen model (Figure 9a). The hyperbola points were extracted and approximated according to Eq. (1) with the use of the Levenberg-Marquardt algorithm (Marquardt 1963) implemented in MATLAB® environment. In the fitting process, a

radius value was set as R = 6 mm. The identified value of electromagnetic wave velocity was 11.86 cm/ns, which in comparison to the real value of 11.4 cm/ns gave a relative error of 4%.

Two linear reflections are visible in the radargram obtained for the model with the vertical joint (Figure 9b). The points with the maximum voltage value were selected. Next, the least squares method was used for the approximation process according to Eq. (2), providing the values v = 15.86 cm/ns (left line) and v = 15.85 cm/ns (right line). The real value for the tested medium was v = 16 cm/ns. Therefore, the estimation error was below 1%.

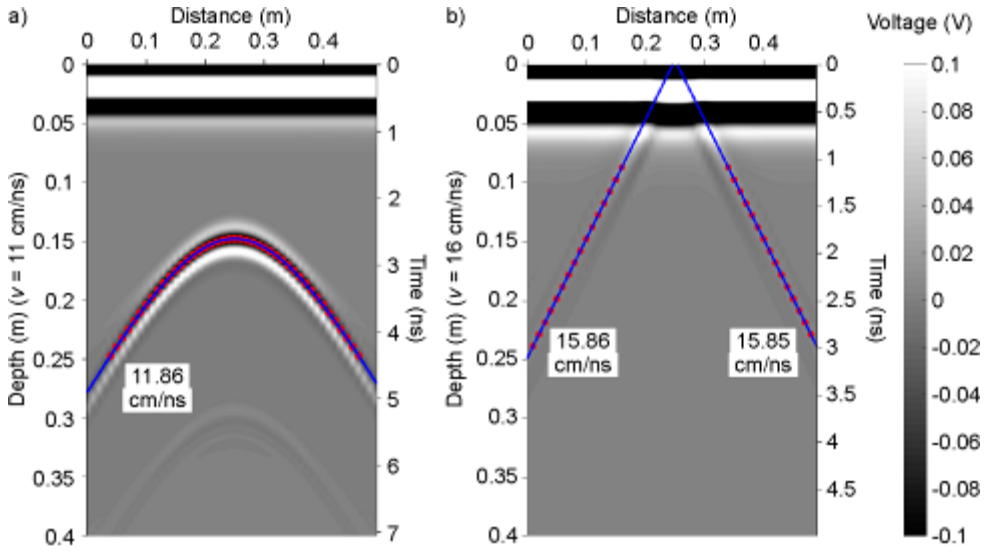

Figure 9. Numerical GPR maps with estimated velocity values based on:
a) hyperbolic diffraction; b) linear diffraction

5. GPR investigations

The GPR surveys were conducted using the Aladdin system manufactured by IDS GeoRadar (Pisa, Italy). An antenna unit operating with a frequency of 2 GHz was used. The distance between the transmitting and receiving antennas was 6 cm. The GPR unit had two sets of antennas with vertical (VV) and horizontal (HH) polarizations. During the research, data from both channels were collected, however, only those from the antenna with horizontal polarization were presented in the results. Registered signals had a two-way time window of 32 ns, and the number of captured samples was 1024 with a step distance of 4 mm. A measuring wheel included in the GPR set was used for measuring the distance interval.

The GPR inspection was conducted on 9 pillars (as highlighted in Figure 2), including 4 brick masonry pillars (M.1 to M.4) and 5 strengthened pillars (S.1 to S.5). The cross section of the pillars was octagonal. The side dimension varied from 50 cm to 67 cm except for two pillars for which the side dimension was larger: 88 cm for pillar M.4 and 98 cm for pillar S.5. On each pillar, longitudinal (L) and transverse (T) scans were acquired. Each transverse scan was composed of eight profiles captured across each side of the octagonal pillar. Additionally,

two or three longitudinal scans (depending on obstacles such as speakers or sculptures) were performed along each side of the pillar.

All experimental GPR maps were processed using the GRED HD software, and then analysed using scripts in the MATLAB® environment. Radargrams were processed using automatic time zero correction and bandpass filtration (500 MHz to 3000 MHz). Finally, a smoothed gain was applied.

6. Results and discussion

5.1. Masonry pillars

The estimation of the electromagnetic wave velocity in the masonry was evaluated based on the surface wave reflected from the joint between bricks according to Eq. (2). In the case of certain pillars, this phenomenon was barely detectable due to the likely small difference in the electrical permeability values of brick and mortar. However, for each pillar in which the phenomenon of the reflected surface wave was found, a linear approximation was made for selected points. The results of the estimation of the wave velocity based on longitudinal GPR maps are shown in Figure 10.

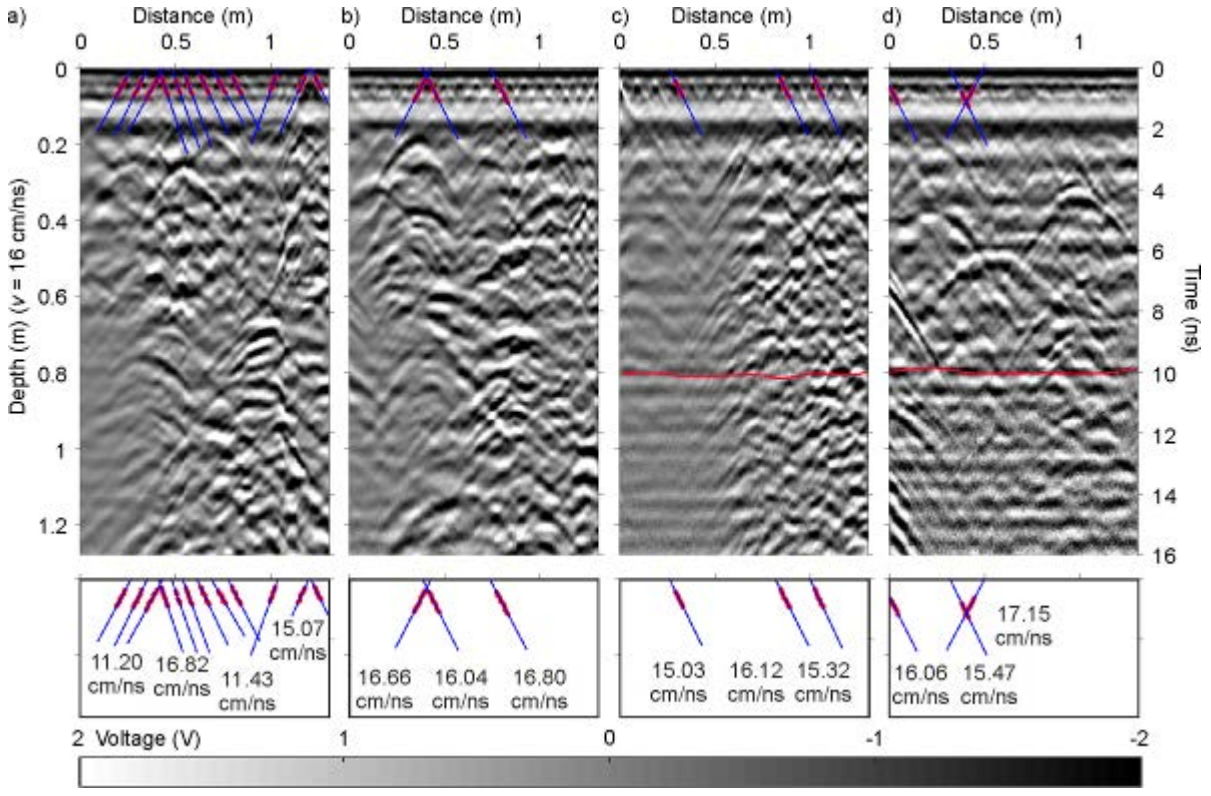

Figure 10. Longitudinal GPR maps with estimated velocity values from measurements of masonry pillars: a) pillar M.1 b) pillar M.2 c) pillar M.3 d) pillar M.4

The average velocity for each pillar fluctuates around 16 cm/ns. A notable phenomenon was observed for pillar M.1, consisting of a change in the wave velocity in certain sections along the pillar height. The drop in the velocity value could be caused by an increase in material moisture, as the electric permittivity that is responsible for the speed of the electromagnetic wave has a much higher value for water (ε_r = 81) than for brick (ε_r = 3.5) (Rucka, Lachowicz, and Zielińska 2016). Moreover, on GPR maps obtained for pillars M.3 and M.4, a longitudinal reflection probably from the end of a layer of bricks can be observed at a delay of approximately 10 ns, indicating that the thickness of this layer can be estimated to be approximately 75 cm based on the estimated velocities. The other reflections appearing on the GPR maps may indicate small air voids or larger elements like bricks or stones.

5.2. Strengthened masonry pillars

To estimate the velocity of electromagnetic waves in the concrete band, the hyperbola fitting method was used. For each strengthened pillar, the nonlinear approximation of selected hyperbolas was performed using the Levenberg-Marquardt algorithm (Marquardt 1963). For each B-scan, three hyperbolas (the least distorted and the most representative) were chosen for the approximation process. The points forming the hyperbola were calculated as the maximum values of the voltage at a given distance from the curve selected a priori on the GPR map. Figure 11 illustrates the longitudinal GPR maps acquired along each strengthened pillar with marked hyperbolas and velocities resulting from the approximation process. For pillars S.1, S.3, S.4 and S.5, similar average values of the velocity (approximately 11.4 cm/ns) were obtained in the approximation process. For pillar S.2, an average velocity of 12.8 cm/ns was determined. According to the identified average velocity values, the time scale was changed into a spatial domain in the longitudinal GPR maps (Figure 11). The velocities obtained based on longitudinal maps were also used for the scale conversion of the transverse maps shown in Figure 12.

In both the longitudinal (Figure 11) and transverse (Figure 12) GPR maps, hyperbolic diffractions indicating reinforcing bars can be observed. To accurately display the reinforcement distribution, the migration processing was performed using the hyperbolic summation method in accordance with the algorithm described earlier. As mentioned before, the velocity value is required for the migration processing. In the conducted investigations, the average velocity of the three hyperbolas (shown in Figure 11) was used for each map. The results of migration are shown in Figure 13 and Figure 14 for longitudinal and transverse scans, respectively. On the migrated GPR maps, the reinforcing bars are clearly represented

by summed points. This type of visualization enables straightforward identification of the depth at which bars are embedded and the spacing between them.

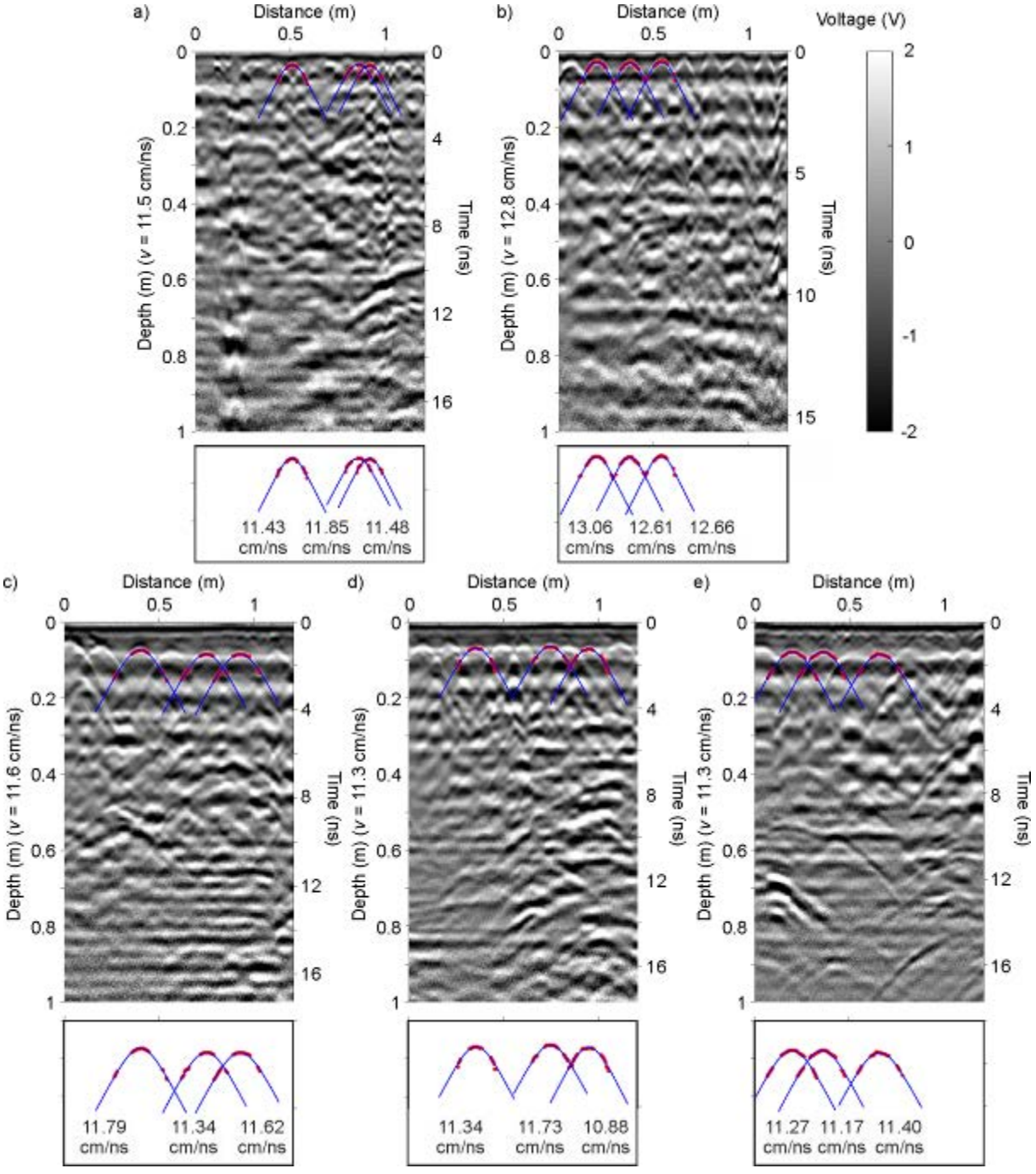

Figure 11. Longitudinal GPR maps with estimated velocity values from measurements of strengthened masonry pillars: a) pillar S.1 b) pillar S.2 c) pillar S.3 d) pillar S.4 e) pillar S.5

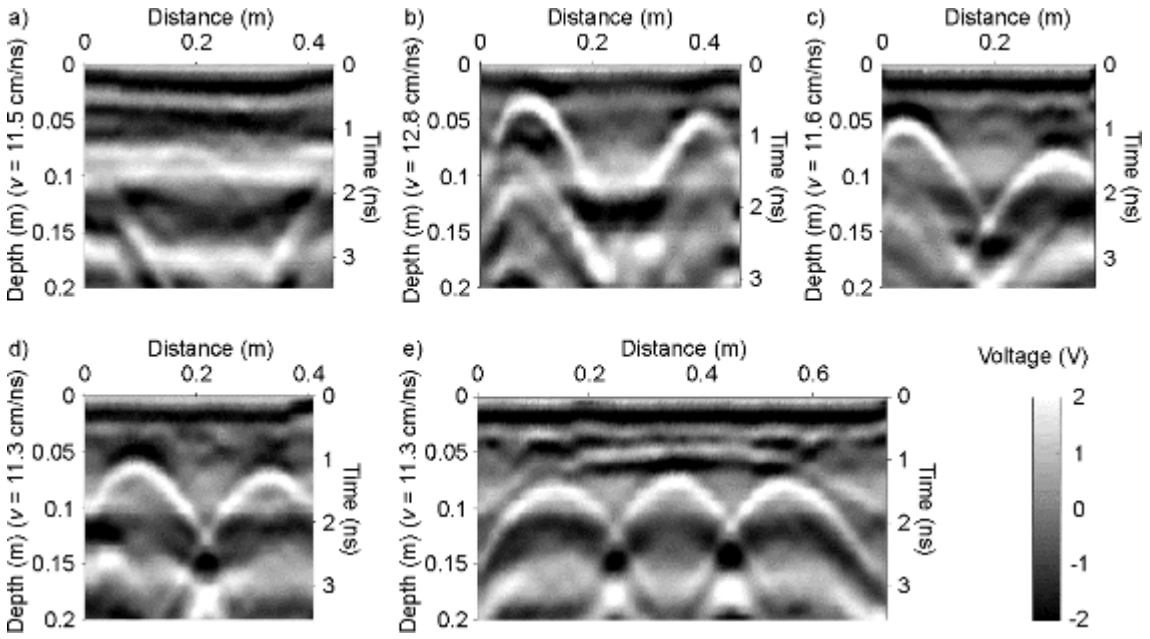

Figure 12. Transverse GPR maps from measurements of strengthened masonry pillars: a) pillar S.1 b) pillar S.2 c) pillar S.3 d) pillar S.4 e) pillar S.5

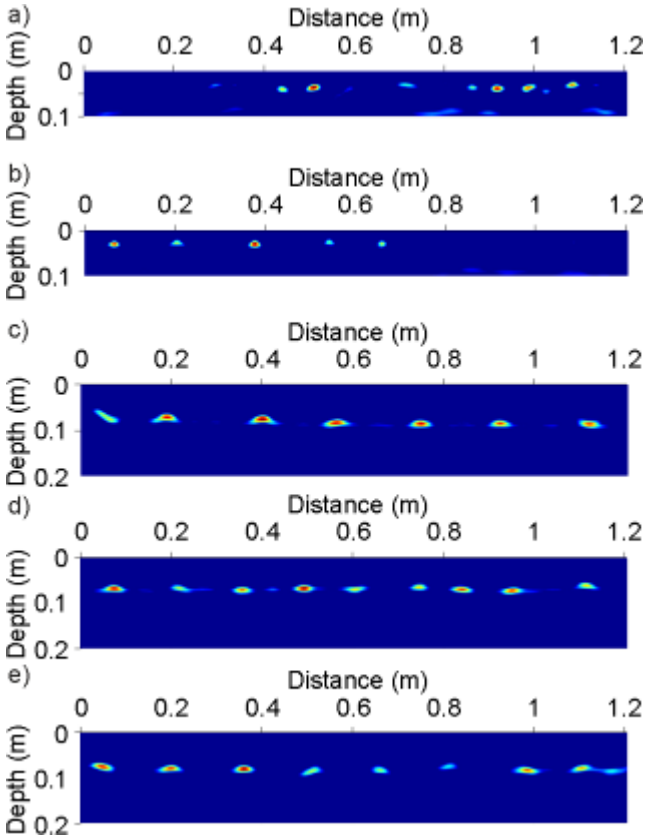

Figure 13. Migrated longitudinal GPR maps: a) pillar S.1; b) pillar S.2; c) pillar S.3; d) pillar S.4; e) pillar S.5

On the basis of the obtained migration results for pillar S.1, reinforcing bars in the transverse direction (across the pillar height) were found to exhibit an average spacing of 10 cm at a depth of approximately 5 cm (Figure 13a). For pillar S.2, the transverse

reinforcement was identified at a depth of approximately 4 cm with an average spacing of 20 cm (Figure 13b). The results for pillar S.3 are shown in Figure 13c, in which transverse bars at a depth of approximately 8 cm with an average spacing of 20 cm are visible. In the case of pillar S.4, it was observed that the transverse reinforcement is located at a denser spacing of approximately 15 cm (Figure 13d). For the largest pillar, S.5, the transverse reinforcement was found at an average spacing of 15 cm at a depth of approximately 8 cm.

The longitudinal reinforcement was identified in the case of four investigated pillars for which monolithic reinforced concrete was used as the strengthening solution. Two bars were found in pillars S.2, S.3 and S.4 with spacing distances of 30 cm, 26 cm and 23 cm, respectively (Figure 14b-d). In the case of pillar S.5, three bars with a spacing of 20 cm can be observed (Figure 14e). No bars in the longitudinal direction were found for pillar S.1 (see Figure 14a and Figure 12) because this pillar was strengthened with the use of prefabricated elements in which reinforcement was applied in only one direction. However, a strong reflection on the migrated GPR map is visible, indicating that the thickness of the reinforced concrete jacket is approximately 10 cm.

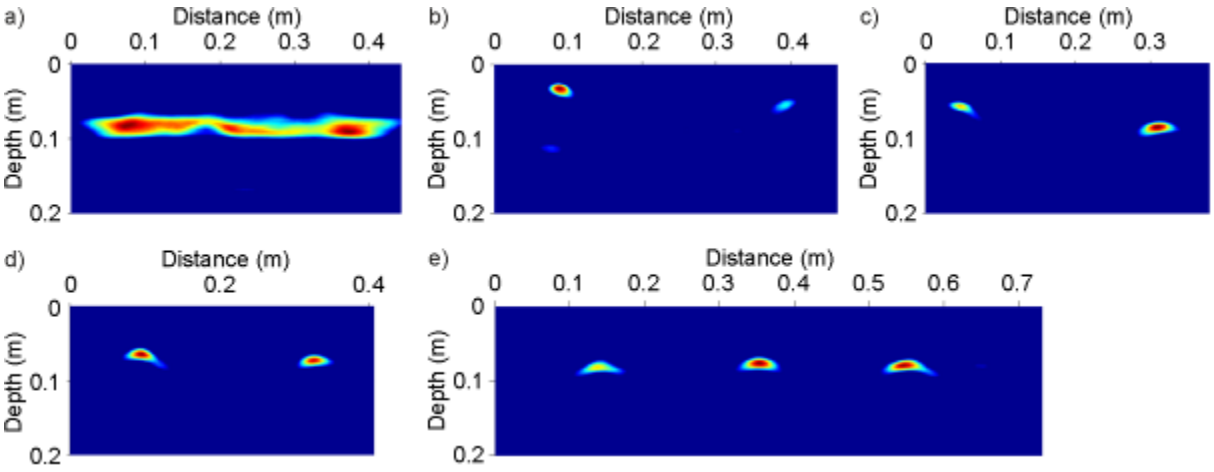

Figure 14. Migrated transverse GPR maps: a) pillar S.1; b) pillar S.2; c) pillar S.3; d) pillar S.4; e) pillar S.5

7. Summary and conclusions

In this study, the GPR method was applied to diagnostics of pillars in St. Mary's Church (Gdańsk, Poland). Four masonry pillars and five pillars strengthened with reinforced concrete jacketing were tested. Conducted investigations focused on the identification of the velocity of electromagnetic waves in both brick and concrete materials, the inspection of the internal structure of pillars and the precise identification of reinforcement bars.

Based on mathematical descriptions of reflection patterns appearing in GPR maps, we estimated the propagation velocity of electromagnetic waves in brick pillars and in pillars

strengthened with a reinforced concrete jacket. In masonry pillars, a novel model based on the line fitting was developed and implemented. The obtained average electromagnetic wave velocity was approximately 16 cm/ns. For one pillar, the identified values exhibited variation along the pillar height, which was attributed to moisture within the material. For this pillar, in the areas of potentially increased moisture, values of approximately 11 cm/ns were obtained. In the case of strengthened pillars, an accurate model including the bar radius and the offset between the receiving and transmitting antennas was applied. As a result of the hyperbola fitting, the average wave propagation velocity was determined to be approximately 11.4 cm/ns for four pillars and 12.8 cm/ns for one pillar.

An inspection of the pillars' internal structure revealed that in the case of masonry pillars, the first layer of bricks had a thickness of approximately 75 cm. For reinforced pillars, it has been established that the concrete jacket had a thickness of 10 cm. The applied hyperbolic summation algorithm enabled precise visualization of the rebar. For all reinforced pillars, transverse bars with a spacing between 15 cm and 20 cm were identified. Longitudinal bars were identified only for pillars reinforced with monolithic concrete.

To summarize, GPR-based diagnostics is suitably efficient for the condition assessment of masonry pillars. The proposed method for identifying the velocity of electromagnetic waves in bricks based on line fitting is expected to be particularly useful in the inspection of historic masonry walls.

References

Binda, L., A. Saisi, C. Tiraboschi, S. Valle, C. Colla, and M. Forde. 2003. "Application of Sonic and Radar Tests on the Piers and Walls of the Cathedral of Noto." *Construction and Building Materials* 17 (8): 613–627. doi:10.1016/S0950-0618(03)00056-4.

Binda, L., A. Saisi, and L. Zanzi. 2003. "Sonic Tomography and Flat-Jack Tests as Complementary Investigation Procedures for the Stone Pillars of the Temple of S. Nicolo 1'Arena (Italy)." *NDT and E International* 36 (4): 215–227. doi:10.1016/S0963-8695(02)00066-X.

Binda, L., L. Zanzi, M. Lualdi, and P. Condoleo. 2005. "The Use of Georadar to Assess Damage to a Masonry Bell Tower in Cremona, Italy." *NDT and E International* 38 (3): 171–179. doi:10.1016/j.ndteint.2004.03.010.

Bogdanowicz, S. 1990. *Sacred Art of the Basilica of St. Mary's Church in Gdańsk.* in Polish. Gdańsk: Stella Maris.

Cetrangolo, G.P., L.D. Domenech, G. Moltini, and A.A. Morquio. 2017. "Determination of Moisture Content in Ceramic Brick Walls Using Ground Penetration Radar." *Journal of Nondestructive Evaluation* 36: 1–12. doi:10.1007/s10921-016-0390-4.

Hamrouche, R., G. Klysz, J.-P. Balayssac, J. Rhazi, and G. Ballivy. 2012. "Numerical Simulations and Laboratory Tests to Explore the Potential of Ground-Penetrating Radar (GPR) in Detecting Unfilled Joints in Brick Masonry Structures." *International Journal*

of Architectural Heritage 6 (6): 648–664. doi:10.1080/15583058.2011.597484.

Hayakawa, H., and A. Kawanaka. 1998. “Radar Imaging of Underground Pipes by Automated Estimation of Velocity Distribution versus Depth.” *Journal of Applied Geophysics* 40: 37–48.

Imposa, S., and G. Mele. 2011. “Ground Penetrating Radar Survey inside the S. Agata Cathedral of Catania (Eastern Sicily).” *International Journal of Architectural Heritage* 5 (2): 188–197. doi:10.1080/15583050903487625.

Júlio, E.S., F. Branco, and V.D. Silva. 2003. “Structural Rehabilitation of Columns with Reinforced Concrete Jacketing.” *Progress in Structural Engineering and Materials* 5 (1): 29–37. doi:10.1002/pse.140.

Lachowicz, J., and M. Rucka. 2018. “3-D Finite-Difference Time-Domain Modelling of Ground Penetrating Radar for Identification of Rebars in Complex Reinforced Concrete Structures.” *Archives of Civil and Mechanical Engineering* 18 (4). Politechnika Wrocławska: 1228–1240. doi:https://doi.org/ 10.1016/j.acme.2018.01.010.

Lai, W.L., T. Kind, S. Kruschwitz, J. Wöstmann, and H. Wiggenhauser. 2014. “Spectral Absorption of Spatial and Temporal Ground Penetrating Radar Signals by Water in Construction Materials.” *NDT and E International* 67. Elsevier: 55–63. doi:10.1016/j.ndteint.2014.06.009.

Leucci, G. 2012. “Ground Penetrating Radar: An Application to Estimate Volumetric Water Content and Reinforced Bar Diameter in Concrete Structures.” *Journal of Advanced Concrete Technology* 10 (12): 411–422. doi:10.3151/jact.10.411.

Leucci, G., R. Cataldo, and G. De Nunzio. 2007. “Assessment of Fractures in Some Columns inside the Crypt of the Cattedrale Di Otranto Using Integrated Geophysical Methods.” *Journal of Archaeological Science* 34 (2): 222–232. doi:10.1016/j.jas.2006.04.012.

Leucci, G., N. Masini, R. Persico, and F. Soldovieri. 2011. “GPR and Sonic Tomography for Structural Restoration: The Case of the Cathedral of Tricarico.” *Journal of Geophysics and Engineering* 8 (3). doi:10.1088/1742-2132/8/3/S08.

Maierhofer, C., and S. Leipold. 2001. “Radar Investigation of Masonry Structures.” *NDT and E International* 34 (2): 139–147. doi:10.1016/S0963-8695(00)00038-4.

Marquardt, D.W. 1963. “An Algorithm for Least-Squares Estimation of Nonlinear Parameters.” *Journal of the Society for Industral and Applied Mathematics* 11 (2): 431–441.

Özdemir, C., Ş. Demirci, and E. Yiğit. 2008. “Practical Algorithms To Focus B-Scan Gpr Images: Theory and Application To Real Data.” *Progress In Electromagnetics Research B* 6: 109–122. doi:10.2528/PIERB08031207.

Özdemir, C., Ş. Demirci, E. Yiğit, and B. Yilmaz. 2014. “A Review on Migration Methods in B-Scan Ground Penetrating Radar Imaging.” *Mathematical Problems in Engineering* 2014 (1): 789–793. doi:10.1155/2014/280738.

Pérez-Gracia, V., J.O. Caselles, J. Clapés, G. Martinez, and R. Osorio. 2013. “Non-Destructive Analysis in Cultural Heritage Buildings: Evaluating the Mallorca Cathedral Supporting Structures.” *NDT and E International* 59. Elsevier: 40–47. doi:10.1016/j.ndteint.2013.04.014.

Pérez-Gracia, V., D. Di Capua, O. Caselles, F. Rial, H. Lorenzo, R. González-Drigo, and J. Armesto. 2011. “Characterization of a Romanesque Bridge in Galicia (Spain).” *International Journal of Architectural Heritage* 5 (3): 251–263.

doi:10.1080/15583050903560249.

Persico, R., G. Leucci, L. Matera, L. De Giorgi, F. Soldovieri, A. Cataldo, G. Cannazza, and E. De Benedetto. 2015. “Effect of the Height of the Observation Line on the the Diffraction Curve in GPR Prospecting.” *Near Surface Geophysics* 13 (3): 243–252. doi:10.3997/1873-0604.2014042.

Ristic, A.V., D. Petrovacki, and M. Govedarica. 2009. “A New Method to Simultaneously Estimate the Radius of a Cylindrical Object and the Wave Propagation Velocity from GPR Data.” *Computers and Geosciences* 35 (8): 1620–1630. doi:10.1016/j.cageo.2009.01.003.

Rucka, M., J. Lachowicz, and M. Zielińska. 2016. “GPR Investigation of the Strengthening System of a Historic Masonry Tower.” *Journal of Applied Geophysics* 131: 94–102. doi:10.1016/j.jappgeo.2016.05.014.

Sagnard, F., and J.-P. Tarel. 2016. “Template-Matching Based Detection of Hyperbolas in Ground-Penetrating Radargrams for Buried Utilities.” *Journal of Geophysics and Engineering* 13 (4). IOP Publishing: 491–504. doi:10.1088/1742-2132/13/4/491.

Santos-Assunçao, S., V. Perez-Gracia, O. Caselles, J. Clapes, and V. Salinas. 2014. “Assessment of Complex Masonry Structures with GPR Compared to Other Non-Destructive Testing Studies.” *Remote Sensing* 6 (9): 8220–8237. doi:10.3390/rs6098220.

Sfarra, S., A. Bendada, C. Ibarra-Castanedo, D. Ambrosini, D. Paoletti, and X. Maldague. 2015. “Santa Maria Di Collemaggio Church (L’Aquila, Italy): Historical Reconstruction by Non-Destructive Testing Techniques.” *International Journal of Architectural Heritage* 9 (4): 367–390. doi:10.1080/15583058.2013.794376.

Sham, J.F.C., and W.W.-L. Lai. 2016. “Development of a New Algorithm for Accurate Estimation of GPR’s Wave Propagation Velocity by Common-Offset Survey Method.” *NDT and E International* 83: 104–113. doi:10.1016/j.ndteint.2016.05.002.

Stryk, J., A.M. Alani, R. Matula, and K. Pospisil. 2015. “Innovative Inspection Procedures for Effective GPR Surveying of Critical Transport Infrastructures (Pavements, Bridges and Tunnels).” In *Civil Engineering Applications of Ground Penetrating Radar*, edited by Andrea Benedetto and Lara Pajewski, 71–95. Springer.

Trojanowska, I., ed. 1997. *Memories of the Reconstruction of the Main City*. in Polish. Marpress.

Warren, C., A. Giannopoulos, and I. Giannakis. 2016. “GprMax: Open Source Software to Simulate Electromagnetic Wave Propagation for Ground Penetrating Radar.” *Computer Physics Communications* 209: 163–170. doi:10.1016/j.cpc.2016.08.020.

Zendri, E., L. Falchi, F.C. Izzo, Z.M. Morabito, and G. Driussi. 2017. “A Review of Common NDTs in the Monitoring and Preservation of Historical Architectural Surfaces.” *International Journal of Architectural Heritage* 11 (7): 987–1004. doi:10.1080/15583058.2017.1331477.